Behavior of Dinonylphenol Phosphate Ester and its influence on the oxidation of a Zn anode in alkaline solution

Deyang Qu *

Department of Chemistry, University of Massachusetts Boston, 100 Morrissey Boulevard, Boston, MA 02125, United States

Abstract

Adsorption and desorption of Dinonylphenol Phosphate Ester (DPE), on the surface of a zinc anode in alkaline solution during discharge, have been studied by *AC* impedance and numerical fitting techniques. The processes were found reversible only during the initial oxidation. The mechanism of the corrosion inhibition caused by the surfactant was investigated and it was found that both the geometrically blocking effect and the increase of hydrogen evolution overpotential might contribute to the reduction of the corrosion rate. The initial potential "dip" during the discharge of an alkaline zinc cell was found to have resulted from surface coverage of the surfactant.
© 2006 Elsevier B.V. All rights reserved.

Keywords: Zinc anode; Dinonylphenol Phosphate Ester; Inhibitor; Alkaline; Initial "dip"; Absorption; Desorption

1. Introduction

Among other significant applications, metallic zinc is widely used as the anode material for primary and secondary batteries in aqueous solution, e.g. alkaline MnO$_2$/Zn and Zn-carbon cells. Zinc has been used as a battery anode material for decades, due to its high specific energy, low cost, abundance and low toxicity. The most important application for zinc anodes is in primary alkaline manganese dioxide cells. In order to achieve a high rate performance in the alkaline electrolyte, the surface area of the zinc anode is increased by suspending zinc powders in gel electrolyte. In the absence of any protective additives, the corrosion of the zinc electrode is the main cause of cell leakage from hydrogen generated by the corrosion process, when the internal pressure is sufficient to burst the safety seal. Amalgamation is the most effective way to suppress zinc corrosion. A few years ago, up to 9% or higher of mercury (by weight) was added in the zinc anode, either by surface or mass amalgamation, to prevent Zn corrosion. Due to environmental concerns, Hg is now banned from use in cylindrical batteries, including zinc-carbon and alkaline primary cells in US and Europe. Amalgamated zinc is still used in button cells, e.g. Zn-air cells for hearing-aid appli-

cations. There has been a great deal of effort to find effective, and environmentally benign inhibitors to replace mercury. Various kinds of additives have been tested as corrosion inhibitors for zinc anodes [1,2], and zinc alloys containing Bi, Pb, In and Al were found with good corrosion resistance [3].

In addition to metallic and inorganic additives, organic inhibitors (surfactants) have also been studied [4–10]. A surfactant is a material that, when dissolved in a solvent, concentrates at the liquid/solid interface. Various kinds of surfactants were tested as corrosion inhibitors, including polyethylene glycols (PEGs), ethoxylated polyfluro-alchol, alkyl polyethylene oxide, diaminepyridine, phenylenediamine, aminonaphthaline sulfonic acid, 2,4-dinitrophenol, benzidine, polyoxyethylene ether, fluorosurfactants, hydroxyethly quinoline quaternary ammonium phenolate, etc. Most of the organic inhibitors have a linear backbone (−O−CH$_2$−CH$_2$−) with different side groups, e.g. phenol groups and various functional groups, e.g. −OH or −POOH.

In the case of the zinc gel electrode, surfactants will coat the surface of zinc particles to form a protective layer. The geometrically blocking effect of adsorbed inhibitive species on the surface of Zn particles can reduce the area of physical contact between the metal and electrolyte. The mechanism of the inhibition effect of a surfactant is still not clear and is under active investigation. Three possible mechanisms have been proposed [5,11,12]: besides the geometrically blocking effect, the inhibition could result from the effect of blocking the active sites on

_____
* Tel.: +1 617 287 6035; fax: +1 617 287 6185.
 E-mail address: Deyang.qu@umb.edu.

the material surface by specific chemisorption, or be due to the electrocatalytic effect of the surfactant resulting from changing the hydrogen evolution overpotential. In addition, the adsorbed species could also have impact both on the kinetic parameters of the charge transfer reaction in zinc oxidation and the geometrical parameters of the interfacial conductive layer, e.g. double-layer and diffusion layer of mass transfer for both zincate ions and OH⁻ ions. The present work is devoted to the investigation of the surface adsorption phenomenon of the organic inhibitor during the Zn oxidation and its impact on electrode discharge kinetics.

Small primary electrochemical cells have been commercially available for many decades. The most widely used primary cells are primary alkaline MnO_2/Zn cells, due to their unique performance characteristics and low manufacturing cost. Recent advances in electronic devices such as digital cameras, MP3 players and high-tech toys, demand much higher electrochemical discharge power than previously attainable. Therefore, to be able to manufacture traditional alkaline cells with better capabilities under high rate conditions would be extremely appealing. Unfortunately, the introduction of organic surfactant inhibitors to replace Hg has a significant impact on the high rate discharge domain for the zinc anode. The high rate performance of a zero Hg zinc anode with (or without) organic inhibitors still needs to be improved in the following areas:

- Initial voltage "dip".
- Voltage "dip" during the high rate oxidation.
- Partial discharge gassing.

2. Experimental method

Zinc electrodes were made by mixing Zn powder with gel electrolyte, using a high-speed lab mixer. UM004 Zinc alloy powders (Umicore, round-shape, Bi/In/Pb = 500/500/500 ppm, with 70% of particles within 150–525 μm by sieving method) were used. In the gel electrolyte, 0.6% polyacrylic acid [13] (Carbopol 940, B.C. Goodrich) was used as the gelling agent, the organic inhibitor was 50 parts Dinonylphenol Phosphate Ester (DPE) [13] (Phone Poulenc RM-510) per million parts Zn, 9 M KOH and 0.5 M ZnO was used as the electrolyte [14].

The zinc anode was housed in an AA cell with a bobbin cathode design. The detailed descriptions of the cell construction have been report elsewhere [15]. The counter cathode contained electrolytic manganese dioxide (K60, EraChem) as the electrochemically active reagent, graphite powder (MP11, NDG) as the conductive filler and KOH solution as the electrolyte. The cathode was made to have intimate contact with the metal to ensure a low ohmic resistivity. A non-woven separator, without surfactant, was placed between the cathode and the anode. The cell was crimp-sealed. The capacity of MnO_2 electrode (8.4 g K60) was significantly higher than that of the zinc electrode (2.4 g Zn alloy), to ensure anode limitation. A hole was carefully drilled in the side of the can into the cathode to reveal the cathode-separator interface; a sealed Zn reference electrode was implanted according to the procedures reported by Barnard et al. [16].

All experiments were done at room temperature (298 ± 1 K).

AC impedance measurements were conducted by means of an AutoLab impedance spectrometer. DC discharge measurements were done with EG&G 170 potentiostat controlled by Q&R Smart Data.

3. Results and discussion

3.1. Theory and equivalent circuits

AC impedance techniques have been successfully applied in the evaluation of corrosion and oxidation of metals with organic coatings [17,18]. The advantage of impedance spectroscopy is acquisition of meaningful mechanistic information, which otherwise could not be obtained through traditional *DC* techniques. Numerical fitting of the impedance spectrum has proved useful for extracting the information. However, most of the equivalent circuits used to simulate coated metal electrodes in the literature were developed under the assumption that the organic or polymer coatings would be strongly attached to the metal surface, without considering the possible effects of desorption. Evidentially, the surfactant adsorbed on the surface of zinc electrode becomes desorbed, during the early stage of oxidation [19,20], and subsequently becomes re-adsorbed.

It is assumed that the surfactant is adsorbed onto the surface of zinc particles. The coverage depends on the type and the percentage content of the surfactant. The electric double layer is established at the electrode/surfactant or electrode/electrolyte interface. ZnO is formed on the Zn surface and beyond the surfactant layer. OH⁻ ions have to cross the surfactant layer and reach the Zn surface in order to facilitate the oxidation. Fig. 1 shows the equivalent circuit used to fit the impedance spectra. Three components in the equivalent circuit represent the interfacial phenomenon of three serial electrochemical processes in the oxidation of a Zn electrode covered with the organic surfactant. R_s is the ohmic resistance of the system, excluding the resistance of the surfactant layer on the surface. The second component is a modified Randles circuit, representing the electrochemical oxidation of the Zn electrode. The oxidation of the zinc electrode can be considered as a surface charge transfer process, with the diffusion of reactants and products to/away from the interface, respectively. The charge transfer process is represented by the charge transfer resistance R_{ct}, while the constant phase element (CPE) is used to simulate the diffusion process for the reactant and product. Due to the formation of the ZnO layer, and thus the
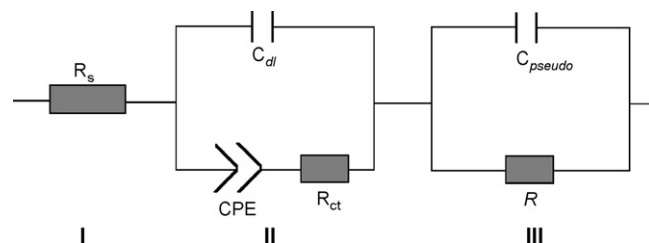

Fig. 1. Equivalent circuit model used in AC impedance fitting. R_s, is the ohmic resistance; C_{dl}, double-layer capacitance; CPE, constant-phase element; R_{ct}, Faraday resistance for Zn oxidation; C_{pseudo}, pseudo capacitance for the adsorbed layer; R, capacitance contributed by the surface adsorption.

non-homogeneity of the Zn surface, the diffusion process cannot be well simulated by Warburg resistance. The impedance of CPE can be represented as [21]:

$$Z = \sigma' \omega^{-m} \left[\cos\left(\frac{1}{2}m\pi\right) - i \sin\left(\frac{1}{2}m\pi\right) \right] \qquad (1)$$

where σ' is said to be the CPE factor and m the CPE exponent. When $m = 0.5$, Eq. (1) stands for Warburg impedance of semi-infinite diffusion and can be written as:

$$Z_w = \sigma(1 - i)\omega^{-1/2} \qquad (2)$$

where Warburg coefficient σ is:

$$\sigma = \frac{V_m}{nFA(2D)^{1/2}} \frac{\partial V_{ocv}}{\partial x} \qquad (3)$$

where D is the diffusion coefficient, $\partial V_{ocv}/\partial x$ is the slope of the open-circuit voltage V_{ocv} versus the mole fraction of Zn. C_{dl} is the double layer capacitance. The third part in the equivalent circuit is a RC component to simulate the surface adsorption layer of surfactant. C_{pseudo} represents the pseudo-capacitance of the adsorption layer and R is its resistance, which could have resulted from the way that the surface adsorption layer impedes the diffusion of reactants to, and products away from, the Zn surface, and ohmic resistance as well. Pseudo-capacitance arises when the potential at which a charge is being passed is a function of the integrated charge accumulated, rather than function of log of current density (Tafel relation), due to special thermodynamic reasons. The pseudo-capacitance is used to represent the electrochemical nature of surfactant adsorption [22]. The surfactant adsorbed on the surface of the Zn electrode could itself be oxidized. Since the zinc surface is initially effectively covered by the surfactant, to reduce the corrosion [8,9,13], the oxidation of Zn electrode is impeded by preventing the physical contact between Zn electrode and electrolyte. The initial kinetics for the coated anode would be determined by the pseudo-capacitance of the surface layer rather than the oxidation of Zn.

3.2. Adsorption and desorption of the surfactant after initial oxidation

Fig. 2A shows the molecular structure of DPE. After the organic surfactant becomes absorbed onto the Zn surface, a thin and compact inhibition layer forms. An affective organic inhibitor should produce full coverage of the Zn surface, to prevent further reaction between Zn and the electrolyte. The length, or backbone, molecular weight, or kinds of side groups and functional groups play very important roles in corrosion inhibition. In the strong alkaline solution, DPE is initially ionized to form the potassium salt as shown in Fig. 2B. It is believed that the interaction between the organic polymer and the zinc is due to the phosphonium functional group. The combination of a strong-bonded site and a linear polymeric chain with 9–11 polyethoxy units will achieve optimal coverage of Zn surface [9].

As mentioned previously, since organic inhibitors were introduced into the zero-Hg Zn anode, a potential "dip" occurs at the very beginning of the high rate discharge of an alkaline pri-
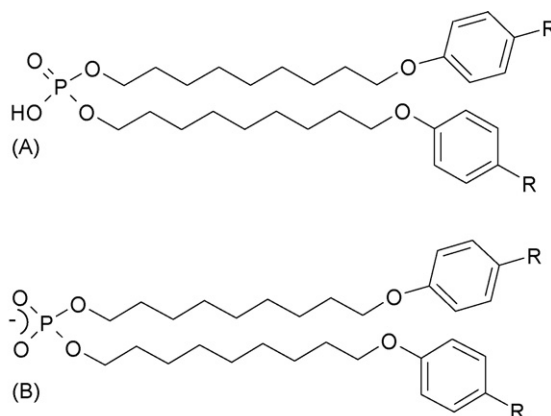

Fig. 2. (A) Chemical formula for Dinonylphenol Phosphate Ester (DPE) and (B) its cation in alkaline solution.

mary cell. As shown in Fig. 3, the Zn electrode potential dipped sharply as soon as anodic polarization current was applied, but subsequently recovered. The initial voltage "dip" could be so significant as to disable commercial electronic devices, by reaching the device "cut-off" voltage, e.g. in an electronic lock used in hotels. Fig. 3 shows the initial 50 s of the oxidation for zinc anodes, with and without the addition of DPE, under a constant current discharge of 1 A. The inset shows the first 500 s of the oxidation for the same electrode. The potential of the anode with the surfactant dipped more than 110 mV from open circuit potential (OCV), as soon as the discharge current was applied. The potential soon recovered about 45 mV within 10 s of continuous oxidation. For the zinc anode without the surfactant, the initial potential dip was about 65 mV (45 mV less than that of the electrode with surfactant) and the potential recovery was less than 5 mV. The initial potential "dip" for the Zn anode without DPE resulted from overpotential and IR drop. In the case of the zinc anode with DPE, the additional 45 mV "dip" ought to be related to the surface phenomena of the surfactant.

Fig. 4 shows the *AC* impedance spectrum for the zinc electrode treated with DPE, before discharge. The impedance was
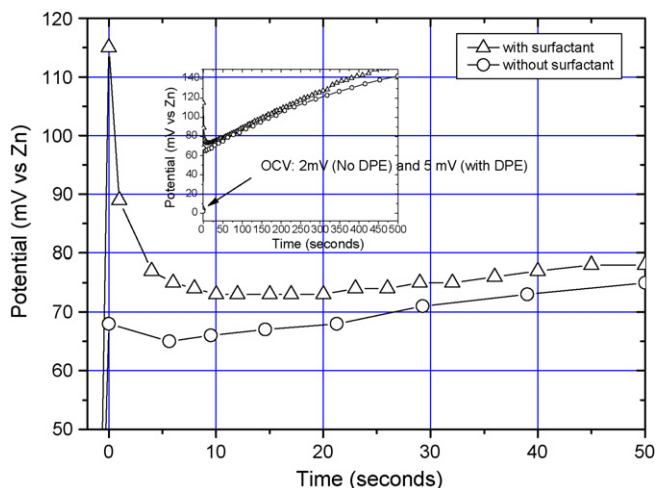

Fig. 3. Comparison of discharge curves for initial 50 s under 1 A constant current discharge for Zn electrodes with and without the addition of the surfactant. The inset shows initial 500 s of the discharge.
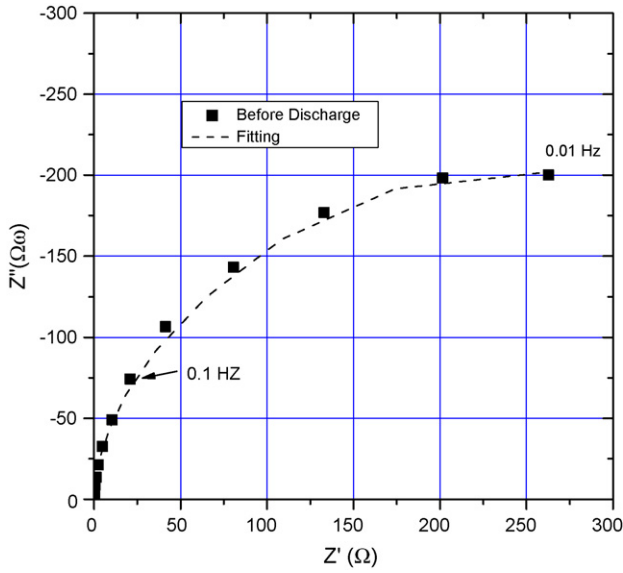
Fig. 4. Comparison of the AC impedance spectrum and fitting results. The impedance was taken on the zinc electrode with surfactant before oxidation at OCV.
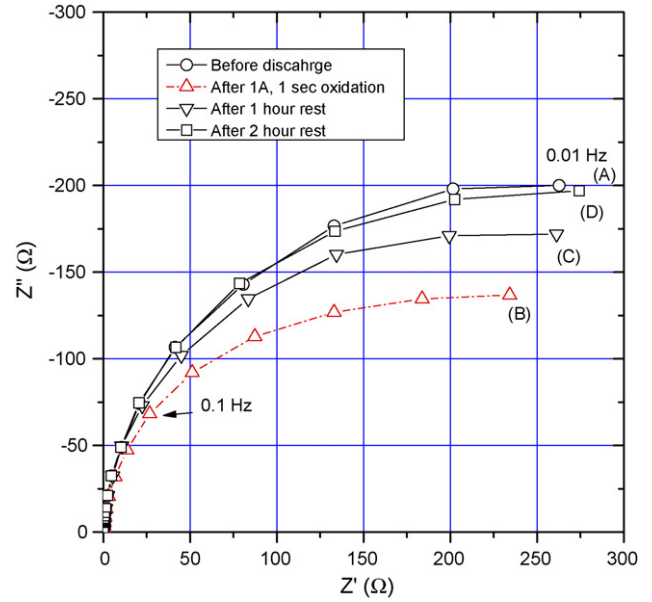

Fig. 5. Comparison of AC impedance spectra for the zinc electrode with surfactant. Before oxidation (A), right after 1 A 1 s discharge (B), after 1 h rest (C) and 2 h rest (D).

measured at OCV, which was about 1 mV versus Zn reference electrode. The fitting results, based on the equivalent circuit shown in Fig. 1, were also plotted in Fig. 4 in comparison with the experimental data. It seems that the experimental results can be well simulated with the equivalent circuit. Fig. 5 shows the *AC* impedance spectra for the same coated zinc electrode. Curve A shows the impedance before oxidation (same as in Fig. 4), curve B shows the impedance of the electrode right after 1 s 1 A anodic polarization, while curves C and D show the electrode impedance, following 1 and 2 h rest after the 1 s 1 A oxidation, respectively. Evidently, the size of the large depressed semi-circle was significantly reduced after the electrode was subjected to a short pulse discharge. During the subsequent rest period, the semi-circle gradually recovered back close to its original shape. Table 1 tabulates the fitting results for all four impedance measurements according to the equivalent circuit shown in Fig. 1. The significant change between curve A and curve B is the sharp reduction of the resistance R (from 417 to 71 Ω). During the rest period, R gradually increased back close to its original value. Since R represents the resistance caused by the surfactant layer adsorbed on the surface of Zn particles, it is reasonable to assume that the adsorption layer became desorbed during the anodic polarization. The desorption process has fast kinetics. The adsorption and desorption processes are reversible, at least

after a short period of anodic polarization. The surfactant can become re-adsorbed on to the surface of zinc particles during the rest period. It is beleived that the geometrically blocking effect on the active Zn surface by the adsorbed surfactant provides significant inhibition, through minimizing the physical contact between the Zn electrode and electrolyte. It is interesting that the changes of pseudo-capacitance were less significant, which may mean that the electrochemical reaction for the surfactant itself is not reversible in the potential range, thus the pseudo-capacitance of the redox reaction of surfactant compound is limited [18]. It is worth pointing out that the resistance R, associated with the absorption layer, is not a simple ohmic resistance, but represents a diffusional resistance in parallel with a pseudo-capacitance, thus its impact on the discharge potential is not explained by the IR drop.

Besides the change of the adsorption layer resistance during discharge and rest periods, the changes of other parameters listed in Table 1 are also worth discussing. The Faraday resistance R_{ct} changed significantly after the initial discharge and subsequent rest period. R_{ct} sharply decreased after the initial discharge and gradually increased to almost half of its initial value. R_{ct} can be used to estimate the inhibition efficiency, the higher the R_{ct} the lower the corrosion current will be. However, it should be

Table 1
Fitting results for *AC* impedance spectra in Fig. 5 based on the equivalent circuit shown in Fig. 1

	Curve A	Curve B	Curve C	Curve D
Ohmic resistance, R_s (Ω)	0.113	0.0874	0.0853	0.0861
Double layer capacitance, C_{dl} (F)	0.0693	0.0206	0.0557	0.152
Faraday resistance, R_{ct} (Ω)	44.51	0.85	20.15	21.05
CPE factor, σ'	–	0.00827	0.00857	–
CPE exponent, m	–	0.223	0.202	–
Pseudo-capacitance, C_{pseudo} (F)	0.0324	0.0853	0.0181	0.0307
Resistance, R (Ω)	417	75	200	412

realized that R_{ct} also determines the polarization overpotential for the oxidation of Zn electrode. The high initial R_{ct} is not only responsible for good corrosion inhibition, but also is partially responsible for the initial potential "dip". The relationship between R_{ct} and the surface coverage may have resulted from the fact that the surfactant could also have an impact on the Zn oxidation reaction mechanism. It may be argued that the change of R_{ct} could simply be caused by the coverage of the active reaction surface. However, when the zinc surface was fully covered again after rest, the R_{ct} only recovered 50% of its original value. Thus, a physical coverage change could not be the reason for the R_{ct} change. Apparently, even though the electrode surface became fully physically covered by the inhibitor, after a prolonged rest, the bonding or molecular level interaction between the surfactant and zinc surface may not be the same, thus the impact on the electrode kinetics is not the same. The phenomenon could be related to the formation of a ZnO layer. Nevertheless, Dinonylphenol Phosphate Ester remarkably increases the charge transfer resistance of the corrosion reaction when it becomes adsorbed on Zn surface, and thus inhibits the corrosion of Zn in alkaline solution.

Ohmic resistance R_s was reduced slightly after the initial anodic oxidation, but remained at the same level during the rest period. The CPE can be ignored, if the Zn surface is totally covered by the surfactant (curves A and D). When the Zn surface is totally covered by the surfactant film, the mass transfer between the electrode surface and the bulk is blocked. For the partially covered surface (curves B and C), m is less than 0.5, the Warburg impedance ($m = 1/2$) could not be applied. The deviation of m from its ideal value ($m = 1/2$) for the Warburg impedance suggests a more complicated phenomenon than purely mass diffusion. It may due to the nature of the porous surface of zinc electrode, the non-homogeneity of the electrode surface and the non-uniform adsorption of the surfactant on the surface of the electrode.

Fig. 6 shows the comparison of the AC impedance spectra for the Zn anode without the surfactant before oxidation, after a 1 A

for 20 s oxidation and after a 2-h rest. It can be observed that the large semi-circle before discharge, in Fig. 5, disappeared. The impedance spectrum is less sensitive to the discharge and subsequent rest, e.g. no distinguishable change can be observed after a 1 A, 1 s oxidation. The change after a 1 A, 20-s oxidation could be result from the dissolution of the surface oxidation layer, which may consist of a low density ZnO or $Zn(OH)_2$. Evidently, the ohmic resistance decreased by 0.5 Ω after oxidation and slightly increased after the 2-h rest. Comparing the results shown in both Figs. 5 and 6, it could be concluded that the phenomena associated with the large semi-circle are surfactant related. It should be emphasized that gassing for cells without a surfactant is much higher than with DPE, and that most of
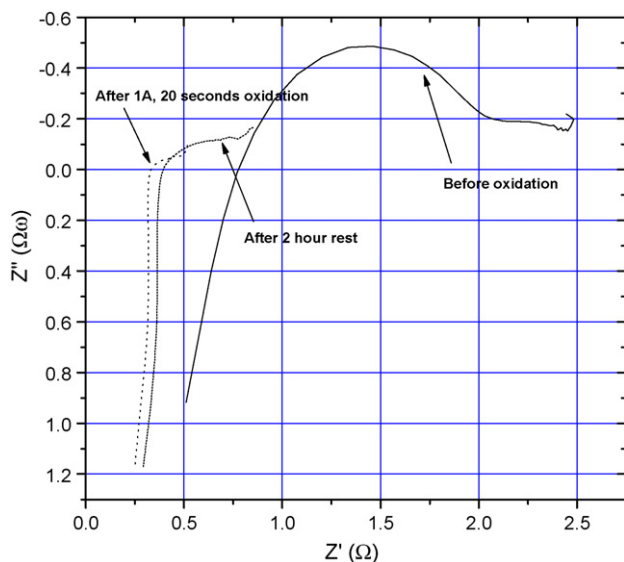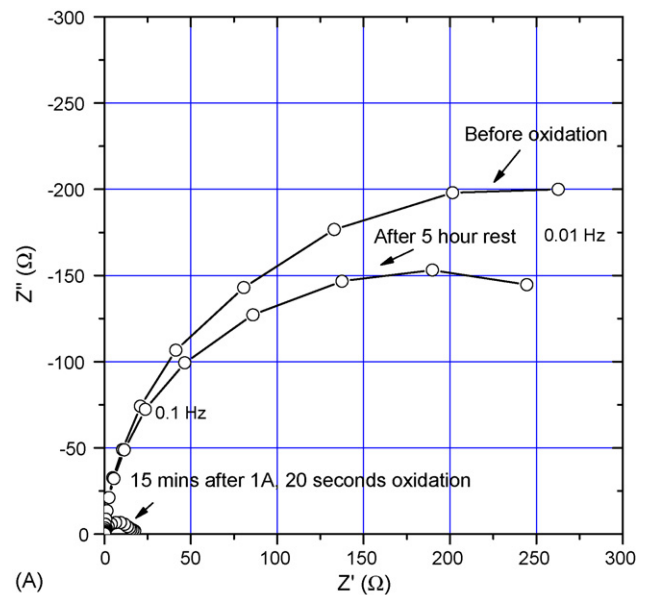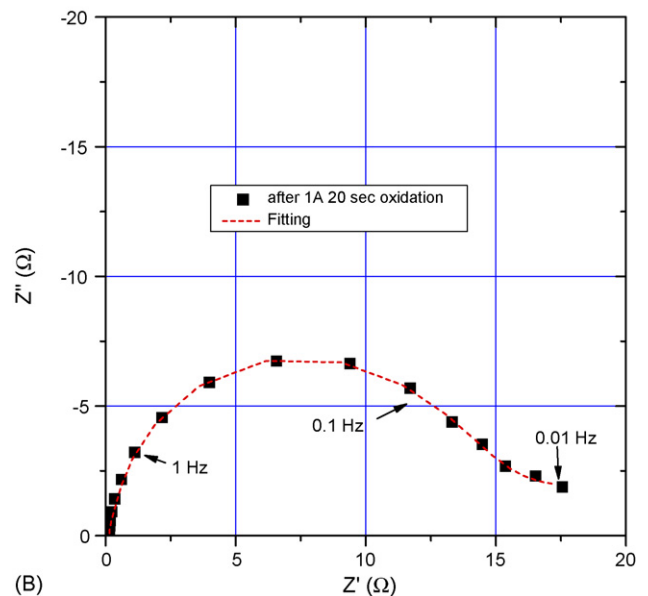

Fig. 6. Comparison of AC impedance spectra for the Zn electrode without the addition of DPE before oxidation, after 1 A 20 s oxidation and after 2 h rest.

Fig. 7. (A) comparison of AC impedance response for the zinc electrode with the surfactant before oxidation, 15 min after 1 A 20 s oxidation and after 5 h rest and (B) comparison of the AC impedance spectrum and fitting results for the Zn electrode with the surfactant 15 min after 1 A 20 s discharge.

Table 2
Fitting results for *AC* impedance spectrum for the Zn electrode with the surfactant after 20 s of 1 A constant current discharge based on the equivalent circuit shown in Fig. 1

	After 1 A 30 s oxidation
Ohmic resistance, R_s (Ω)	0.143
Double layer capacitance, C_{dl} (F)	0.0190
Faraday resistance, R_{ct} (Ω)	0.50
CPE factor, σ'	0.0737
CPE exponent, m	0.185
Pseudo-capacitance, C_{pseudo} (F)	0.0693
Resistance, R (Ω)	0.3342

cells made, especially those partially discharged, leaked during storage.

3.3. The conditions of the Zn electrode surface after prolonged oxidation

Fig. 7A shows a comparison of the impedance spectra for the Zn electrode before oxidation, discharged at 1 A constant current for 20 s and after 5 h rest. The potential in the discharge curve can be totally recovered from the "dip" after 20 s during a 1 A oxidation as shown in Fig. 3. Almost all the surfactant on the electrode surface should become desorbed by then. The large depressed semi-circle, associated with RC$_{pseudo}$, disappeared. The impedance spectrum, after 20 s of a 1A discharge, should only relate to the electrochemical reaction of zinc electrode. Fig. 6B shows the comparison of the fitting results and the experimental data, while Table 2 lists the fitting parameters. The significant reduction of R (Table 2) from its original value before the oxidation (Table 1) also demonstrates that the surfactant on the electrode surface became desorbed. The low Faraday resistance (R_{ct}) demonstrates that

the zinc electrode can be oxidized with a low overpotential.

During the rest period, the desorbed surfactant can become adsorbed again onto the electrode surface (the depressed semi-circle reappeared after rest). However, it should be observed that the surface of the electrode can only become partially covered, even after the prolonged rest. The length of discharge seems to have an effect on the activity of the surfactant. After being galvanostatically discharged, under 1A for 20 min, the surfactant was permanently de-activated and could not be re-adsorbed back onto the electrode surface, even after resting for 10 days. Fig. 8 shows the comparison of the impedance spectra of the zinc electrode, 10 days after 1 A 20 min discharge and 10 days after another 1 A 20 min discharge. The deactivation mechanism is still not clear and is under active investigation.

Evidentially, Dinonylphenol Phosphate Ester may serve well as an inhibitor initially, but its effectiveness becomes gradually diminished during discharge, which may be partially responsible for the high gassing of alkaline MnO$_2$/Zn cells after partial discharge.

4. Conclusions

The adsorption and desorption, and inhibition mechanism for zinc corrosion, of a Dinonylphenol Phosphate Ester surfactant on the surface of a zinc anode in alkaline solution have been investigated. The following points should be noted:

1. Inhibition of the surfactant for the zinc corrosion is partially due to a geometrical blocking effect. The surfactant can effectively cover the surface of the Zn electrode, which prevents physical contact between the electrolyte and electrode.
2. The surfactant adsorbed on the surface may also change the overpotential for zinc oxidation.
3. The surfactant can become desorbed during the initial anodic polarization (<10 s).
4. Adsorption and desorption are reversible only in the very initial stage (∼15 min at 1A discharge) of discharge. After prolonged oxidation, the process becomes irreversible. This is partially responsible for the high partial discharge gassing of alkaline zinc cells.
5. Based on these results, the initial potential "dip" in alkaline Zn cells with the addition of surfactants, is believed to be due to the surface adsorption of surfactants.
6. A good organic inhibitor for the zinc anode used in alkaline batteries should be a surfactant which has fast kinetics for desorption during anodic polarization and has a tendency to become adsorbed, even after prolonged oxidation.
7. The disappearance of re-adsorption of the surfactant is still under investigation, the hypothesis is that it could be due to the reaction of the surfactant or the formation of a ZnO layer.
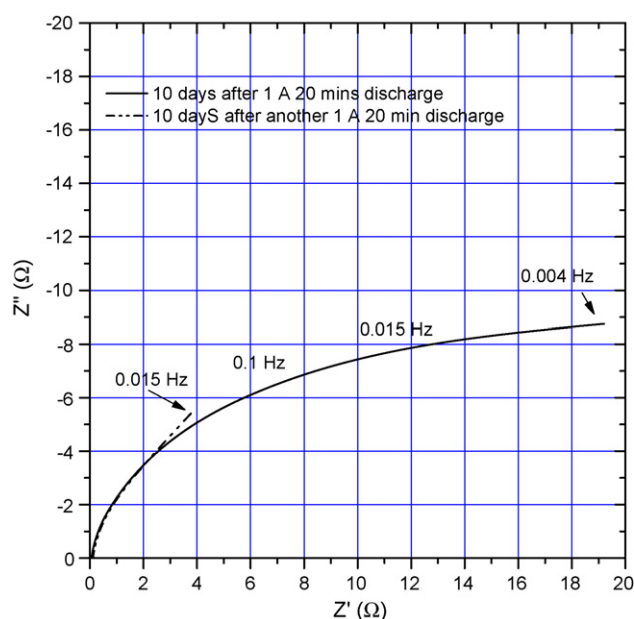

Fig. 8. Comparison of the AC impedance response (solid line) 10 day after 1 A 20 min oxidation; (dash line) 10 days after another 1 A 20 min oxidation.

References

[1] T.S. Lee, J. Electrochem. Soc. 120 (1973) 707.
[2] T.S. Lee, J. Electrochem. Soc. 122 (1975) 171.
[3] J.Y. Huot, E. Boubour, J. Power Sources 65 (1997) 81.

[4] C. Cachel, R. Wiart, Electrochim. Acta 44 (1999) 4743.

[5] J.M. Wang, Y. Lu, J. Zhang, C. Cao, Corros. Sci. 40 (1998) 1161.

[6] J.L. Zhu, Y.H. Zhou, C.Q. Gao, J. Power Sources 72 (1998) 231.

[7] S. Manov, A.M. Lanazouere, L. Aries, Corros. Sci. 42 (2000) 1235.

[8] Y. Ein-Eli, M. Auinat, D. Starosvetsky, J. Power Sources 114 (2003) 330.

[9] Y. Ein-Eli, M. Auinat, J. Electrochem. Soc. 150 (2003), A1606 and A1614.

[10] M. Auinat, Y. Ein-Eli, J. Electrochem. Soc. 152 (2005) A1158.

[11] C. Cao, Corros. Sci. 38 (1996) 2073.

[12] W.J. Lorenz, F. Mansfeld, Proceedings of the Sixth Symposium European Inhibition of Corrosion, University of Ferrara, Ferrara, 1985, p. 23.

[13] William W. Yen, *WO 99/53555*.

[14] M.J. Root, J. Appl. Electrochem. 25 (1995) 1057.

[15] D.Y. Qu, D. Diehl, B.E. Conway, W.G. Pell, S.Y. Qian, J. Appl. Electrochem. 35 (2005) 1111.

[16] R. Barnard, L.M. Baugh, C.F. Randell, J. Appl. Electrochem. 17 (1987) 165.

[17] F. Mansfeld, M. Kendig, S. Tsai, Corrosion 38 (1982) 478.

[18] M. Kendig, F. Mansfeld, S. Tsai, Corros. Sci. 23 (1983) 122.

[19] J.M. Wang, Y.D. Qian, J.Q. Zhang, C.N. Cao, J. Appl. Electrochem. 30 (2000) 113.

[20] D. Zhang, L.D. Li, L.X. Cao, N.F. Yang, C.B. Huang, Corros. Sci. 43 (2001) 1627.

[21] C. Ho, I.D. Rastrick, R.A. Hugins, J. Electrochem. Soc. 127 (1980) 343.

[22] D.Y. Qu, J. Power Sources 109 (2002) 403.